

Reinforced Imitation Learning by Free Energy Principle

Ryoya Ogishima¹ Izumi Karino¹ Yasuo Kuniyoshi¹

Abstract

Reinforcement Learning (RL) requires a large amount of exploration especially in sparse-reward settings. Imitation Learning (IL) can learn from expert demonstrations without exploration, but it never exceeds the expert's performance and is also vulnerable to distributional shift between demonstration and execution. In this paper, we radically unify RL and IL based on Free Energy Principle (FEP). FEP is a unified Bayesian theory of the brain that explains perception, action and model learning by a common fundamental principle. We present a theoretical extension of FEP and derive an algorithm in which an agent learns the world model that internalizes expert demonstrations and at the same time uses the model to infer the current and future states and actions that maximize rewards. The algorithm thus reduces exploration costs by partially imitating experts as well as maximizing its return in a seamless way, resulting in a higher performance than the suboptimal expert. Our experimental results show that this approach is promising in visual control tasks especially in sparse-reward environments.

1. Introduction

Reinforcement Learning (RL) autonomously explores to maximize rewards, even achieving super-human performances in certain tasks(Sutton et al., 1998; Silver et al., 2016). It can also transfer the acquired policy to new tasks/environments with additional explorations. However, in realistic tasks, RL often requires an excess amount of explorations especially in sparse-reward settings, and even when it succeeds in reward maximization, the acquired policy sometimes severely deviates from the intention of the reward designer.

Imitation Learning (IL) learns a policy to mimic the trajectories demonstrated by an expert(Pomerleau, 1991). Therefore

it does not require explorations nor a careful design of a reward function. However, the policy acquired by IL never exhibits the performance exceeding that of the suboptimal expert, and it is also vulnerable to realistic setting with distributional shift between the demonstration and execution environments or perturbation and noise.

Since the pros and cons of RL and IL are mutually compensating, a natural consequence would be to combine the two methods. Several work have been reported along this idea (Verma et al., 2019; Pfeiffer et al., 2018; Sun et al., 2018b; Rhinehart et al., 2018). However, there still remains an important problem. That is, a truly seamless unification of IL and RL on a common theoretical ground to make the best out of mutual leverages, and dealing with another realistic setting which is partial observability as in POMDP (Partially Observable Markov Decision Process), particularly with high-dimensional image inputs. It is widely assumed that introducing a generative model of the world in terms of latent variables is a promising approach to POMDP.

Recent work in model-based RL succeeds in latent planning from high-dimensional image inputs by incorporating latent dynamics models. Behaviors can be derived either by imagined-reward maximization (Ha & Schmidhuber, 2018; Hafner et al., 2019a) or by online planning (Hafner et al., 2019b). Although solving high dimensional visual control tasks with model-based methods is becoming feasible, prior methods have not been combined with IL.

Free Energy Principle (FEP), a unified brain theory in computational neuroscience explains perception, action and model learning in a Bayesian probabilistic way (Friston et al., 2006; Friston, 2010). In FEP, the brain has a generative model of the world and computes a mathematical amount called Free Energy using the model prediction and sensory inputs to the brain. By minimizing the Free Energy, the brain achieves model learning and behavior learning. Therefore it has a potential to fundamentally unify IL and RL on the common theoretical ground. However, prior work on FEP dealt with limited situations where a part of the generative model is given and the task is very low dimensional. As there are a lot in common between FEP and variational inference in machine learning, recent advancements in deep learning and latent variable models could be applied to scale up FEP agents to be compatible with high dimensional tasks.

¹Graduate School of Information Science and Technology, The University of Tokyo, Tokyo, Japan. Correspondence to: Ryoya Ogishima <ogishima@isi.imi.i.u-tokyo.ac.jp>.

In this paper, we propose Deep Free Energy Network (FENet), an agent that combines the advantages of IL and RL so that the initial policy is learned from suboptimal expert data without the need of exploration or detailed reward crafting, then it is further improved from sparsely specified reward functions to exceed the suboptimal expert performance.

The key contributions of this work are summarized as follows:

- **Extension of Free Energy Principle:**

We theoretically extend Free Energy Principle, introducing policy prior and policy posterior to combine IL and RL. We implement the proposed method on top of Recurrent State Space Model (Hafner et al., 2019b), a latent dynamics model with both deterministic and stochastic components.

- **Visual control tasks in realistic problem settings:**

We solve Cheetah-run, Walker-walk, and Quadruped-walk tasks from DeepMind Control Suite (Tassa et al., 2018). We do not only use the default problem settings, but we also set up problems with sparse rewards and with suboptimal experts. We demonstrate that our agent outperforms model-based RL using Recurrent State Space Model in sparse-reward settings. We also show that our agent can achieve higher returns than Behavioral Cloning (IL) with suboptimal experts.

2. Backgrounds on Free Energy Principle

2.1. Problem setups

We formulate visual control as a partially observable Markov decision process (POMDP) with discrete time steps t , observations o_t , hidden states s_t , continuous action vectors a_t , and scalar rewards r_t . The goal is to develop an agent that maximizes expected return $\mathbb{E}[\sum_{t=1}^T r_t]$.

2.2. Free Energy Principle

Perception, action and model learning are all achieved by minimizing the same objective function, Free Energy (Friston et al., 2006; Friston, 2010). In FEP, the agent is equipped with a generative model of the world, using a prior $p(s_t)$ and a likelihood $p(o_t|s_t)$.

$$p(o_t, s_t) = p(o_t|s_t)p(s_t) \quad (1)$$

Perceptual Inference Under the generative model, the posterior probability of hidden states given observations is calculated with Bayes' theorem as follows.

$$p(s_t|o_t) = \frac{p(o_t|s_t)p(s_t)}{p(o_t)}, \quad p(o_t) = \int p(o_t|s_t)p(s_t)ds \quad (2)$$

Since we cannot compute $p(o_t)$ due to the integral, we think of approximating $p(s_t|o_t)$ with a variational posterior $q(s_t)$ by minimizing KL divergence $KL(q(s_t)||p(s_t|o_t))$.

$$KL(q(s_t)||p(s_t|o_t)) = \ln p(o_t) + KL(q(s_t)||p(o_t, s_t)) \quad (3)$$

$$F_t = KL(q(s_t)||p(o_t, s_t)) \quad (4)$$

The Free Energy is defined as (eq.4). Since $p(o_t)$ does not depend on s_t , we can minimize (eq.3) w.r.t. the parameters of the variational posterior by minimizing the Free Energy. Thus, the agent can infer the hidden states of the observations by minimizing F_t . This process is called 'perceptual inference' in FEP.

Perceptual Learning Free Energy is the same amount as negative Evidence Lower Bound (ELBO) in variational inference often seen in machine learning as follows.

$$\ln p(o_t) \geq -F_t \quad (5)$$

By minimizing F_t w.r.t. the parameters of the prior and the likelihood, the generative model learns to best explain the observations. This process is called 'perceptual learning' in FEP.

Active Inference We can assume that the prior is conditioned on the hidden states and actions at the previous time step as follows.

$$p(s_t) := p(s_t|s_{t-1}, a_{t-1}) \quad (6)$$

The agent can change the future by choosing actions. Suppose the agent chooses a_t when it is at s_t , the prior can predict the next hidden state s_{t+1} . Thus, we can think of the Expected Free Energy G_{t+1} at the next time step $t+1$ as follows (Friston et al., 2015).

$$\begin{aligned} G_{t+1} &= \mathbb{E}_{p(o_{t+1}|s_{t+1})}[KL(q(s_{t+1})||p(o_{t+1}, s_{t+1}))] \\ &= \mathbb{E}_{q(s_{t+1})p(o_{t+1}|s_{t+1})}[\ln q(s_{t+1}) - \ln p(o_{t+1}, s_{t+1})] \end{aligned} \quad (7)$$

$$\begin{aligned} &= \mathbb{E}_{q(s_{t+1})p(o_{t+1}|s_{t+1})}[\ln q(s_{t+1}) - \ln p(s_{t+1}|o_{t+1}) \\ &\quad - \ln p(o_{t+1})] \\ &\approx \mathbb{E}_{q(o_{t+1}, s_{t+1})}[\ln q(s_{t+1}) - \ln q(s_{t+1}|o_{t+1}) \\ &\quad - \ln p(o_{t+1})] \end{aligned} \quad (8)$$

$$\begin{aligned} &= \mathbb{E}_{q(o_{t+1})}[-KL(q(s_{t+1}|o_{t+1})||q(s_{t+1})) \\ &\quad - \ln p(o_{t+1})] \end{aligned} \quad (9)$$

Since the agent has not experienced time step $t+1$ yet and has not received observations o_{t+1} , we take expectation over o_{t+1} using the likelihood $p(o_{t+1}|s_{t+1})$ as (eq.7). In (eq.8), we define the likelihood $q(o_{t+1}|s_{t+1}) = p(o_{t+1}|s_{t+1})$ and approximate the posterior $p(s_{t+1}|o_{t+1})$ as the variational posterior $q(s_{t+1}|o_{t+1})$. According to the complete class

theorem (Friston et al., 2012), any scalar rewards can be encoded as observation priors using $p(o) \propto \exp r(o)$ and the second term in (eq.9) becomes a goal-directed value. This observation prior $p(o_{t+1})$ can also be regarded as the probability of optimality variable $p(\mathcal{O}_{t+1} = 1|o_{t+1})$, where the binary optimality variable $\mathcal{O}_{t+1} = 1$ denotes that time step $t + 1$ is optimal and $\mathcal{O}_{t+1} = 0$ denotes that it is not optimal as introduced in the context of control as probabilistic inference(Levine, 2018). The first term in (eq.9) is called epistemic value that works as intrinsic motivation to further explore the world. Minimization of $-KL(q(s_{t+1}|o_{t+1})||q(s_{t+1}))$ means that the agent tries to experience as different states s_{t+1} as possible given some imagined observations o_{t+1} . By minimizing the Expected Free Energy, the agent can infer the actions that explores the world and maximize rewards. This process is called ‘active inference’.

3. Deep Free Energy Network (FENet)

Perceptual learning deals with learning the generative model to best explain the agent’s sensory inputs. If we think of not only observations but also actions demonstrated by the expert as a part of the sensory inputs, we can explain IL by using the concept of perceptual learning. In other words, this is a process of learning the world model that internalizes expert demonstrations as passive dynamics. Active inference deals with exploration and reward maximization, so it is compatible with reinforcement learning. By minimizing the same objective function, the Free Energy, we can deal with both IL and RL.

In this section, we first extend the Free Energy so that actions are a part of the sensory inputs to accommodate both IL and RL. For this purpose, we introduce a policy prior for IL and a policy posterior for RL. Second, we use the extended Free Energy to derive and extend the Expected Free Energy in two ways. One is for calculation with given expert data for IL, and the other is for calculation with collected agent data for RL. Finally, we explain a detailed network design to implement the proposed method for solving image control tasks.

3.1. Introducing a policy prior and a policy posterior

Free Energy We extend the Free Energy from (eq.4) so that actions are a part of the sensory inputs that the generative model tries to explain.

$$F_t = KL(q(s_t)||p(o_t, s_t, a_t)) \quad (10)$$

$$= KL(q(s_t)||p(o_t|s_t)p(a_t|s_t)p(s_t|s_{t-1}, a_{t-1})) \quad (11)$$

$$= \mathbb{E}_{q(s_t)}[\ln \frac{q(s_t)}{p(o_t|s_t)p(a_t|s_t)p(s_t|s_{t-1}, a_{t-1})}] \quad (12)$$

$$= \mathbb{E}_{q(s_t)}[-\ln p(o_t|s_t) - \ln p(a_t|s_t) + \ln q(s_t)]$$

$$- \ln p(s_t|s_{t-1}, a_{t-1})] \quad (13)$$

$$= \mathbb{E}_{q(s_t)}[-\ln p(o_t|s_t) - \ln p(a_t|s_t) \\ + KL(q(s_t)||p(s_t|s_{t-1}, a_{t-1})) \quad (14)$$

We define $p(a_t|s_t)$ as a policy prior. When the agent observes expert trajectories, by minimizing F_t w.r.t. the policy prior parameters, the policy prior will be learned so that it can best explain the experts. By minimizing F_t w.r.t. the parameters of the state prior $p(s_t|s_{t-1}, a_{t-1})$ and the observation likelihood $p(o_t|s_t)$, the world model is learned as explained as perceptual learning in Section 2.2. Besides the policy prior, we introduce and define a policy posterior $q(a_t|s_t)$, which is the very policy that the agent samples actions from when interacting with its environments and that the agent uses to imagine the future observations and rewards. We explain how to learn the policy posterior in the following.

Expected Free Energy for Imitation Learning (IL) In a similar manner to active inference in Section 2.2, we think of the Expected Free Energy G_{t+1} at the next time step $t + 1$, but this time we take expectation over the policy posterior $q(a_t|s_t)$ because G_{t+1} is a value expected under the next actions. Note that in Section 2.2 a_t was given as a certain value input, but here a_t is sampled from the policy posterior. We calculate the expected state at time step $t + 1$ as follows.

$$q(s_{t+1}) = \mathbb{E}_{q(s_t)q(a_t|s_t)}[p(s_{t+1}|s_t, a_t)] \quad (15)$$

$$q(o_{t+1}, s_{t+1}, a_{t+1}) = p(o_{t+1}|s_{t+1})q(a_{t+1}|s_{t+1})q(s_{t+1}) \quad (16)$$

We derive the Expected Free Energy from (eq.13) as follows.

$$G_{t+1}^{IL} = \mathbb{E}_{q(o_{t+1}, s_{t+1}, a_{t+1})}[-\ln p(o_{t+1}|s_{t+1}) \\ - \ln p(a_{t+1}|s_{t+1}) + \ln q(s_{t+1}) - \ln p(s_{t+1}|s_t, a_t)] \quad (17)$$

$$= \mathbb{E}_{q(o_{t+1}, s_{t+1}, a_{t+1})}[-\ln p(o_{t+1}|s_{t+1}) \\ - \ln p(a_{t+1}|s_{t+1}) + 0] \quad (18)$$

$$= \mathbb{E}_{q(o_{t+1}, s_{t+1})}[-\ln p(o_{t+1}|s_{t+1}) \\ + \mathbb{E}_{q(a_{t+1}|s_{t+1})}[-\ln p(a_{t+1}|s_{t+1})]] \quad (19)$$

$$= \mathbb{E}_{q(s_{t+1})}[\mathcal{H}[p(o_{t+1}|s_{t+1})] \\ + \mathbb{E}_{q(a_{t+1}|s_{t+1})}[-\ln p(a_{t+1}|s_{t+1})]] \quad (20)$$

In (eq.18), $q(s_{t+1})$ and $p(s_{t+1}|s_t, a_t)$ are both state prior prediction at future time step $t + 1$, and they are regarded as the same value. In (eq.20), the first term is the entropy of the observation likelihood, and the second term is the negative likelihood of the policy prior expected under the policy posterior. By minimizing G_{t+1}^{IL} , the agent learns the policy posterior so that it matches the policy prior which has been learned through minimizing F_t to encode the experts’ behavior.

Expected Free Energy for RL We can get the Expected Free Energy in a different way that has a reward component

$r(o_{t+1})$ leading to the policy posterior maximizing rewards. We derive the Expected Free Energy from (eq.17) as follows.

$$G_{t+1}^{RL} = \mathbb{E}_{q(o_{t+1}, s_{t+1}, a_{t+1})} [-\ln p(o_{t+1}, s_{t+1}) - \ln p(a_{t+1}|s_{t+1}) + \ln q(s_{t+1})] \quad (21)$$

$$= \mathbb{E}_{q(o_{t+1}, s_{t+1}, a_{t+1})} [-\ln p(s_{t+1}|o_{t+1}) - \ln p(a_{t+1}|s_{t+1}) + \ln q(s_{t+1}) - \ln p(o_{t+1})] \quad (22)$$

$$\approx \mathbb{E}_{q(o_{t+1}, s_{t+1}, a_{t+1})} [-\ln q(s_{t+1}|o_{t+1}) - \ln p(a_{t+1}|s_{t+1}) + \ln q(s_{t+1}) - \ln p(o_{t+1})] \quad (23)$$

$$= \mathbb{E}_{q(o_{t+1}, s_{t+1})} [-\ln q(s_{t+1}|o_{t+1}) - \ln p(o_{t+1}) + \mathbb{E}_{q(a_{t+1}|s_{t+1})} [-\ln p(a_{t+1}|s_{t+1})] + \ln q(s_{t+1})] \quad (24)$$

$$= \mathbb{E}_{q(o_{t+1})} [-KL(q(s_{t+1}|o_{t+1})||q(s_{t+1})) - \ln p(o_{t+1}) + \mathbb{E}_{q(s_{t+1})} [\mathbb{E}_{q(a_{t+1}|s_{t+1})} [-\ln p(a_{t+1}|s_{t+1})]]] \quad (25)$$

$$\approx \mathbb{E}_{q(o_{t+1})} [-KL(q(s_{t+1}|o_{t+1})||q(s_{t+1})) - r(o_{t+1}) + \mathbb{E}_{q(s_{t+1})} [\mathbb{E}_{q(a_{t+1}|s_{t+1})} [-\ln p(a_{t+1}|s_{t+1})]]] \quad (26)$$

In (eq.23), we approximate $p(s_{t+1}|o_{t+1})$ as $q(s_{t+1}|o_{t+1})$ similarly to (eq.8). This is to approximate true state posterior as variational state posterior. In (eq.26), as is explained in active inference in Section 2.2, we use $p(o) \propto \exp r(o)$ for the approximation. The first KL term is the epistemic value that lets the agent explore the world, the second term is the expected reward under the action sampled from the policy posterior, and the last term is the likelihood of the policy prior expected under the policy posterior. Note that $q(o_{t+1})$ in (eq.26) can be calculated as follows.

$$q(o_{t+1}) = \mathbb{E}_{q(s_{t+1})} [p(o_{t+1}|s_{t+1})] \quad (27)$$

By minimizing G_{t+1}^{RL} , the agent learns the policy posterior so that it explores the world and maximizes the reward as long as it does not deviate too much from the policy prior which has encoded experts' behavior through minimizing F_t .

In summary, G_{t+1}^{IL} and G_{t+1}^{RL} are both derived from the same Free Energy F_t , but they are different kinds of derivations to accommodate the data inputs required for IL and RL respectively.

3.2. IL and RL objectives

To realize IL and RL at the same time, we propose that the agent calculate Free Energy-based losses for given expert data and collected agent data. The overall loss function of Deep Free Energy Network should minimize is as follows.

$$\mathcal{F}_{IL} + \mathcal{F}_{RL} \quad (28)$$

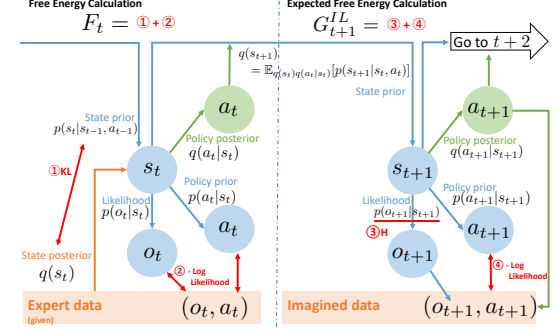


Figure 1. Deep Free Energy Network (FENet) calculation process for IL phase.

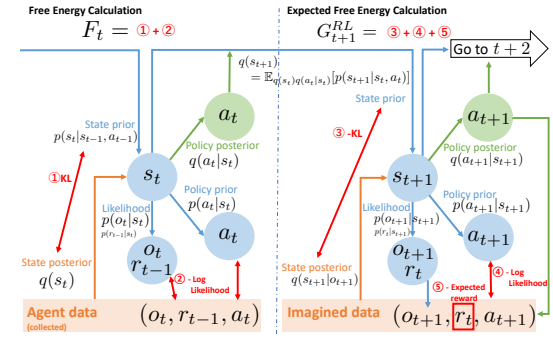


Figure 2. Deep Free Energy Network (FENet) calculation process for RL phase.

when, for given expert data,

$$\mathcal{F}_{IL} = F_t + \sum_{\tau=t+1}^{\infty} \gamma^{\tau-t-1} G_{\tau}^{IL} \quad (29)$$

for collected agent data,

$$\mathcal{F}_{RL} = F_t + \sum_{\tau=t+1}^{\infty} \gamma^{\tau-t-1} G_{\tau}^{RL} \quad (30)$$

Note that the Expected Free Energy at $t+1$ to ∞ are calculated to account for the long term future and that γ is a discount factor as in the case of general RL algorithms. The overall Free Energy calculation process is shown in Figure 1 and Figure 2.

3.3. Network Design for Implementation

Value function As it is impossible to sum over infinity time steps, we introduce an Expected Free Energy Value function $V(s_{t+1})$ to estimate the cumulative Expected Free Energy. Similarly to the case of Temporal Difference learning of Deep Q Network (Mnih et al., 2013), we use a target

network $V_{targ}(s_{t+2})$ to stabilize the learning process and define the loss for learning the value function as follows.

$$\mathcal{L} = \|G_{t+1} + \gamma V_{targ}(s_{t+2}) - V(s_{t+1})\|^2 \quad (31)$$

To reduce the number of parameters of the networks, we made a design choice that the agent uses the value function only for RL, and not for IL. In IL, we use only the value of the Expected Free Energy G_{t+1} at the next time step $t+1$ and ignore the time steps from $t+2$ to infinity. Note that we use a notation that the origin of time step t is set at the time of the expert data the agent learns from in every iteration of learning. This means that the time steps from $t+1$ to infinity are all imagined time because the agent has not observed the time yet. Therefore, IL from $F_t + G_{t+1}^{IL}$ without $t+2$ to infinity still handles all time series data of expert demonstrations. It just does not predict more than 1 time step ahead. While IL can be achieved without long term prediction, RL needs the value function to predict rewards in the long-term future to avoid a local minimum behavior and achieve the desired goal.

Recurrent State Space Model We made a design choice for the network implementation to use Recurrent State Space Model (Hafner et al., 2019b), a latent dynamics model with both deterministic and stochastic components. In this model, the hidden states s_t are split into two parts: stochastic hidden states u_t and deterministic hidden states h_t . The deterministic transition of h_t is modeled using Recurrent Neural Networks (RNN) f as follows.

$$h_t = f(h_{t-1}, u_{t-1}, a_{t-1}) \quad (32)$$

We model the probabilities in Deep Free Energy Networks as follows.

$$\text{State prior} \quad p_\theta(u_t|h_t) \quad (33)$$

$$\text{Observation likelihood} \quad p_\theta(o_t|u_t, h_t) \quad (34)$$

$$\text{Reward likelihood} \quad p_\theta(r_{t-1}|u_t, h_t) \quad (35)$$

$$\text{State posterior} \quad q_\phi(u_t|h_t, o_t) \quad (36)$$

$$\text{Policy prior} \quad p_\theta(a_t|u_t, h_t) \quad (37)$$

$$\text{Policy posterior} \quad q_\psi(a_t|u_t, h_t) \quad (38)$$

$$\text{Value network} \quad V_\omega(u_t) \quad (39)$$

$$\text{Target Value Network} \quad V_{\omega_{targ}}(u_t) \quad (40)$$

We model these probabilities as feedforward Neural Networks that output the mean and standard deviation of the random variables according to the Gaussian distribution. For example, the policy posterior is modeled as a network that takes u_t and h_t as inputs and calculates through several hidden layers and outputs the Gaussian distribution of a_t . Note that $\theta, \phi, \psi, \omega$ are a group or set of network parameters to be learned such as network weights. For example, θ is a group or set of all parameters consisting the probabilities

of state prior, observation/reward likelihood and policy prior. Using the network parameters, the objective loss functions can be written as follows.

$$\mathcal{F}_{IL} = F_t + G_{t+1}^{IL} \quad (41)$$

$$\mathcal{F}_{RL} = F_t + G_{t+1}^{RL} + \gamma V_{\omega_{targ}}(u_{t+2}) \quad (42)$$

$$\mathcal{L} = \|G_{t+1}^{RL} + \gamma V_{\omega_{targ}}(u_{t+2}) - V_\omega(u_{t+1})\|^2 \quad (43)$$

when

$$\begin{aligned} F_t &= \mathbb{E}_{q_\phi(u_t|h_t, o_t)}[-\ln p_\theta(o_t|u_t, h_t) - \ln p_\theta(a_t|u_t, h_t)] \\ &\quad + KL(q_\phi(u_t|h_t, o_t)||p_\theta(u_t|h_t)) \end{aligned} \quad (44)$$

$$\begin{aligned} G_{t+1}^{IL} &= \mathbb{E}_{q(u_{t+1})}[\mathcal{H}[p_\theta(o_{t+1}|u_{t+1}, h_{t+1})] \\ &\quad + KL(q_\psi(a_{t+1}|u_{t+1}, h_{t+1})||p_\theta(a_{t+1}|u_{t+1}, h_{t+1}))] \end{aligned} \quad (45)$$

$$\begin{aligned} G_{t+1}^{RL} &= \mathbb{E}_{q(o_{t+1})}[-KL(q_\phi(u_{t+1}|h_{t+1}, o_{t+1})||q(u_{t+1})) \\ &\quad - p_\theta(r_t|u_{t+1}, h_{t+1})] + \mathbb{E}_{q(u_{t+1})}[\\ &\quad KL(q_\psi(a_{t+1}|u_{t+1}, h_{t+1})||p_\theta(a_{t+1}|u_{t+1}, h_{t+1})) \\ &\quad + \gamma V_{\omega_{targ}}(u_{t+2})] \end{aligned} \quad (46)$$

$$q(u_{t+1}) = \mathbb{E}_{q_\phi(u_t|h_t, o_t)q_\psi(a_t|u_t, h_t)}[p_\theta(u_{t+1}|h_{t+1})] \quad (47)$$

$$q(o_{t+1}) = \mathbb{E}_{q(u_{t+1})}[p_\theta(o_{t+1}|u_{t+1}, h_{t+1})] \quad (48)$$

Algorithm 1 shows overall calculations using these losses. The agent minimizes \mathcal{F}_{IL} for expert data \mathcal{D}_E and the agent minimizes \mathcal{F}_{RL} for agent data \mathcal{D}_A that the agent collects on its own.

4. Experiments

We evaluate FENet on three continuous control tasks from images. We compare our model with model-based RL and model-based RL with demonstrations in dense and sparse reward setting when optimal expert is available. Then we compare our model with IL methods when only suboptimal experts are available. Finally, we investigate the merits of combining IL and RL as an ablation study.



Figure 3. Image-based control tasks used in our experiments.

Control tasks We used Cheetah-run, Walker-walk, and Quadruped-walk tasks, image-based continuous control tasks of DeepMind Control Suite (Tassa et al., 2018) shown in Figure 3. The agent gets rewards ranging from 0 to 1. Quadruped-walk is the most difficult as it has more action

dimensions than the others. Walker-walk is more challenging than Cheetah-run because an agent first has to stand up and then walk, meaning that the agent easily falls down on the ground, which is difficult to predict. The episode length is 1000 steps starting from randomized initial states. We use action repeat $R = 4$ for the Cheetah-run task, and $R = 2$ for the Walker-walk task and the Quadruped-walk task.

4.1. Performance in standard visual control tasks

We compare the performance of FENet to PlaNet (Hafner et al., 2019b) and "PlaNet with demonstrations" in standard visual control tasks mentioned above. We use PlaNet as a baseline method because PlaNet is one of the most basic model-based RL methods using Recurrent State Space Model, on top of which we build our model. As FENet uses expert data, we create "PlaNet with demonstrations" for fair comparison. This variant of PlaNet has an additional experience replay pre-populated with expert trajectories and minimize a loss calculated from the expert data in addition to PlaNet's original loss. Figure 4 shows that "PlaNet with demonstrations" is always better than PlaNet and that FENet is ranked higher as the difficulty of tasks gets higher. In Cheetah-run, FENet gives competitive performance with PlaNet. In Walker-walk, FENet and "PlaNet with demonstrations" are almost competitive, both of which are substantially better than PlaNet thanks to expert knowledge being leveraged to increase sample efficiency. In Quadruped-walk, FENet is slightly better than the other two baselines.

4.2. Performance in sparse-reward visual control tasks

In real-world robot learning, it is demanding to craft a dense reward function to lead robots to desired behaviors. It would be helpful if an agent could acquire desired behaviors simply by giving sparse signals. We compare the performance of FENet to PlaNet and "PlaNet with demonstrations" in sparse-reward settings, where agents do not get rewards less than 0.5 per time step (Note that in the original implementation of Cheetah-run, Walker-walk and Quadruped-walk, agents get rewards ranging from 0 to 1 per time step). Figure 5 shows that FENet outperforms PlaNet and "PlaNet with demonstrations" in all three tasks. In Cheetah-run, PlaNet and "PlaNet with demonstrations" are not able to get even a single reward.

4.3. Performance with suboptimal experts

In real-world robot learning, expert trajectories are often given by human experts. It is natural to assume that expert trajectories are suboptimal and that there remains much room for improvement. We compare the performance of FENet to Behavioral Cloning IL methods. We use two types of networks for behavioral cloning methods: recurrent policy and recurrent decoder policy. The recurrent policy

$\pi_R(a_t|o_t)$ is neural networks with one gated recurrent unit cell and three dense layers. The recurrent decoder policy $\pi_R(a_t, o_{t+1}|o_t)$ is neural networks with one gated recurrent unit cell and four dense layers and deconvolution layers as in the decoder of PlaNet. Both networks does not get raw pixel observations but take observations encoded by the same convolutional encoder as PlaNet's. Figure 7 shows that while IL methods overfit to the expert and cannot surpass the suboptimal expert performance, FENet is able to substantially surpass the suboptimal expert's performance.

Algorithm 1 Deep Free Energy Network (FENet)

Input:	
Seed episodes S	Collect interval C
Batch size B	Chunk length L
Expert episodes N	Target smoothing rate ρ
Learning rate α	
State prior $p_\theta(u_t h_t)$	State posterior $q_\phi(u_t h_t, o_t)$
Policy prior $p_\theta(a_t u_t, h_t)$	Policy posterior $q_\psi(a_t u_t, h_t)$
Likelihood $p_\theta(o_t u_t, h_t)$, $p_\theta(r_{t-1} u_t, h_t)$	
Value function $V_\omega(u_t)$	Target value function $V_{\omega_{targ}}(u_t)$

```

Initialize expert dataset  $\mathcal{D}_E$  with  $N$  expert trajectories
Initialize agent dataset  $\mathcal{D}_A$  with  $S$  random episodes
Initialize neural network parameters  $\theta, \phi, \psi, \omega$  randomly
while not converged do
    for update step  $c = 1..C$  do
        // Imitation Learning (IL)
        Draw expert data  $\{(o_t, a_t, o_{t+1})_{t=k}^{k+L}\}_{i=1}^B \sim \mathcal{D}_E$ 
        Compute Free Energy  $\mathcal{F}_{IL}$  from equation 41
        // Reinforcement Learning (RL)
        Draw agent data  $\{(o_t, a_t, r_t, o_{t+1})_{t=k}^{k+L}\}_{i=1}^B \sim \mathcal{D}_A$ 
        Compute Free Energy  $\mathcal{F}_{RL}$  from equation 42
        Compute  $V$  function's Loss  $\mathcal{L}$  from equation 43
        // Update parameters
         $\theta \leftarrow \theta - \alpha \nabla_\theta (\mathcal{F}_{IL} + \mathcal{F}_{RL})$ 
         $\phi \leftarrow \phi - \alpha \nabla_\phi (\mathcal{F}_{IL} + \mathcal{F}_{RL})$ 
         $\psi \leftarrow \psi - \alpha \nabla_\psi (\mathcal{F}_{IL} + \mathcal{F}_{RL})$ 
         $\omega \leftarrow \omega - \alpha \nabla_\omega \mathcal{L}$ 
         $\omega_{targ} \leftarrow \rho \omega_{targ} + (1 - \rho) \omega$ 
    end for
    // Environment interaction
     $o_1 \leftarrow \text{env.reset}()$ 
    for time step  $t = 1..T$  do
        Infer hidden states  $u_t \leftarrow q_\phi(u_t|h_t, o_t)$ 
        Calculate actions  $a_t \leftarrow q_\psi(a_t|u_t, h_t)$ 
        Add exploration noise to actions
         $r_t, o_{t+1} \leftarrow \text{env.step}(a_t)$ 
    end for
     $\mathcal{D}_A \leftarrow \mathcal{D}_A \cup \{(o_t, a_t, r_t, o_{t+1})_{t=1}^T\}$ 
end while

```

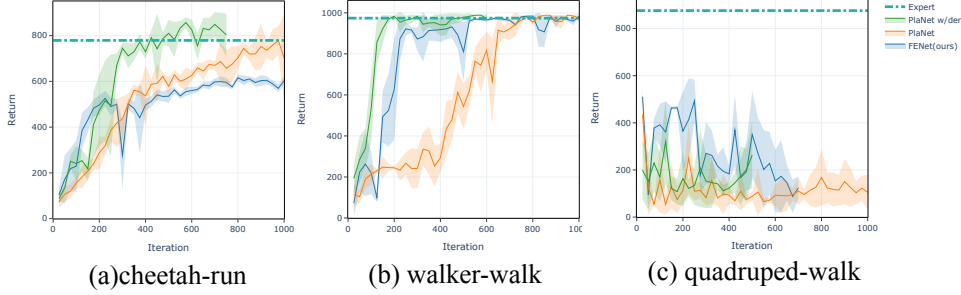


Figure 4. Comparison of FENet to PlaNet and "PlaNet with demonstrations". Plots show test performance over learning iterations. The lines show means and the areas show standard deviations over 10 trajectories.

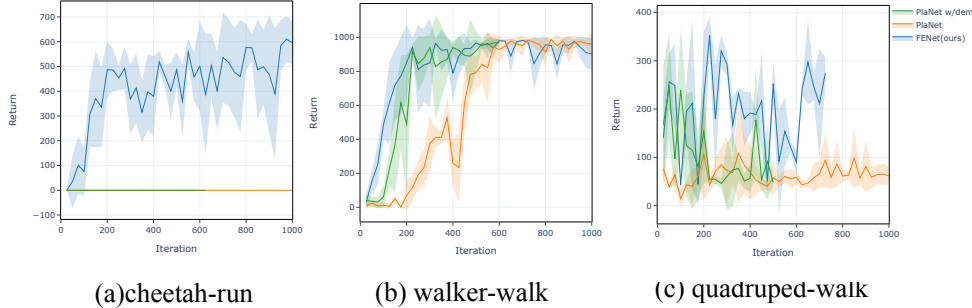


Figure 5. Comparison of FENet to PlaNet and "PlaNet with demonstrations" in sparse-reward settings, where agents do not get rewards less than 0.5. Plots show test performance over learning iterations. FENet substantially outperforms PlaNet. The lines show means and the areas show standard deviations over 10 trajectories.

4.4. Ablation Study

Figure 6 compares FENet with other types of agents partially using FENet's loss in Cheetah-run and Walker-walk (ablation study). 'Imitation RL' is the proposed FENet agent that does IL and RL at the same time, minimizing $\mathcal{F}_{IL} + \mathcal{F}_{RL}$. 'Imitation-pretrained RL' is an agent that first learns the model only with imitation (minimizing \mathcal{F}_{IL}) and then does RL using the pre-trained model (minimizing \mathcal{F}_{RL}). 'RL only' is an agent that does RL only, minimizing \mathcal{F}_{RL} . 'Imitation only' is an agent that does IL only, minimizing \mathcal{F}_{IL} . While 'Imitation only' gives the best performance and 'Imitation RL' gives the second best in Cheetah-run, 'Imitation RL' gives the best performance and 'Imitation only' gives the worst performance in Walker-walk. We could say 'Imitation RL' is the most robust to the properties of tasks.

5. Related Work

Active Inference Friston, who first proposed Active Inference, has evaluated the performance in simple control tasks and a low-dimensional maze (Friston et al., 2012;

2015). Ueltzhoffer implemented Active Inference with Deep Neural Networks and evaluated the performance in a simple control task (Ueltzhöffer, 2018). Millidge proposed a Deep Active Inference framework with value functions to estimate the correct Free Energy and succeeded in solving Gym environments (Millidge, 2019). Our approach extends Deep Active Inference to combine IL and RL, solving more challenging tasks.

RL from demonstration Reinforced Imitation Learning succeeds in reducing sample complexity by using imitation as pre-training before RL (Pfeiffer et al., 2018). Adding demonstrations into a replay buffer of off policy RL methods also demonstrates high sample efficiency (Vecerik et al., 2017; Nair et al., 2018; Paine et al., 2019). Demo Augmented Policy Gradient mixes the policy gradient with a behavioral cloning gradient (Rajeswaran* et al., 2018). Deep Q-learning from Demonstrations (DQfD) not only use demonstrations for pre-training but also calculates gradients from demonstrations and environment interaction data (Hester et al., 2018). Truncated HORIZON Policy Search uses demonstrations to shape rewards so that subsequent plan-

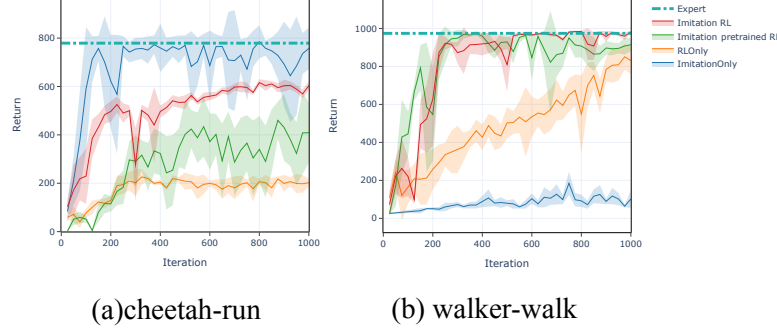


Figure 6. Comparison of FENet (imitation RL) to partial FENet (as ablation studies: Imitation-pretrained RL, RL only, and Imitation only). Plots show test performance over learning iterations. The lines show means and the areas show standard deviations over 10 trajectories.

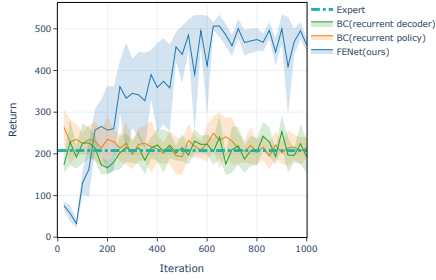


Figure 7. Comparison of FENet to IL methods when only suboptimal experts are available in Cheetah-run. Plots show test performance over learning iterations. Behavioral Cloning IL methods cannot surpass the suboptimal expert’s return which FENet successfully surpasses. The lines show means and the areas show standard deviations over 10 trajectories.

ning can achieve superior performance to RL even when experts are suboptimal (Sun et al., 2018a). Soft Q Imitation Learning gives rewards that encourage the agent to return to demonstrated states in order to avoid policy collapse (Reddy et al., 2019). Our approach is similar to DQfD in terms of mixing gradients calculated from demonstrations and from environment interaction data. One key difference is that FENet concurrently learns the generative model of the world so that it can be robust to wider environment properties.

Control with latent dynamics model World Models acquire latent spaces and dynamics over the spaces separately, and evolve simple linear controllers to solve visual control tasks (Ha & Schmidhuber, 2018). PlaNet learns Recurrent State Space Model and does planning with Model Predictive Control at test phase (Hafner et al., 2019b). Dreamer, which is recently built upon PlaNet, has a policy for latent imagination and achieved higher performance than PlaNet

(Hafner et al., 2019a). Our approach also uses Recurrent State Space Model to describe variational inference, and we are the first to unify IL and RL over latent dynamics models to the best of our knowledge.

6. Conclusion

We present FENet, an agent that unifies Imitation Learning (IL) and Reinforcement Learning (RL) using Free Energy objectives. For this, we theoretically extend the Free Energy Principle and introduce a policy prior that encodes experts’ behaviors and a policy posterior that learns to maximize expected rewards without deviating too much from the policy prior. FENet outperforms model-based RL and RL with demonstrations especially in visual control tasks with sparse rewards and FENet also outperforms suboptimal experts’ performance unlike Behavioral cloning. Strong potentials in sparse environment with suboptimal experts are important factors for real-world robot learning.

Directions for future work include learning the balance between IL and RL, i.e. Free Energy and Expected Free Energy so that the agent can select the best approach to solve its confronting tasks by monitoring the value of Free Energy. It is also important to evaluate FENet in real-world robotic tasks to fully manifest its effectiveness and reveal demands for further improvements.

References

- Friston, K. The free-energy principle: a unified brain theory? *Nature reviews neuroscience*, 11(2):127–138, 2010.
- Friston, K., Kilner, J., and Harrison, L. A free energy principle for the brain. *Journal of Physiology-Paris*, 100 (1-3):70–87, 2006.
- Friston, K., Samothrakis, S., and Montague, R. Active infer-

- ence and agency: optimal control without cost functions. *Biological cybernetics*, 106(8-9):523–541, 2012.
- Friston, K., Rigoli, F., Ognibene, D., Mathys, C., Fitzgerald, T., and Pezzulo, G. Active inference and epistemic value. *Cognitive neuroscience*, 6(4):187–214, 2015.
- Ha, D. and Schmidhuber, J. World models. *arXiv preprint arXiv:1803.10122*, 2018.
- Haarnoja, T., Zhou, A., Abbeel, P., and Levine, S. Soft actor-critic: Off-policy maximum entropy deep reinforcement learning with a stochastic actor. In *International conference on machine learning*, pp. 1861–1870. PMLR, 2018.
- Hafner, D., Lillicrap, T., Ba, J., and Norouzi, M. Dream to control: Learning behaviors by latent imagination. *arXiv preprint arXiv:1912.01603*, 2019a.
- Hafner, D., Lillicrap, T., Fischer, I., Villegas, R., Ha, D., Lee, H., and Davidson, J. Learning latent dynamics for planning from pixels. In Chaudhuri, K. and Salakhutdinov, R. (eds.), *Proceedings of the 36th International Conference on Machine Learning*, volume 97, pp. 2555–2565, Long Beach, California, USA, 2019b. PMLR.
- Hester, T., Vecerik, M., Pietquin, O., Lanctot, M., Schaul, T., Piot, B., Horgan, D., Quan, J., Sendonaris, A., Osband, I., et al. Deep q-learning from demonstrations. In *Thirty-Second AAAI Conference on Artificial Intelligence*, 2018.
- Kapturowski, S., Ostrovski, G., Dabney, W., Quan, J., and Munos, R. Recurrent experience replay in distributed reinforcement learning. In *International Conference on Learning Representations*, 2019.
- Kingma, D. P. and Ba, J. Adam: A method for stochastic optimization. *arXiv preprint arXiv:1412.6980*, 2014.
- Levine, S. Reinforcement learning and control as probabilistic inference: Tutorial and review. *arXiv preprint arXiv:1805.00909*, 2018.
- Millidge, B. Deep active inference as variational policy gradients. *arXiv preprint arXiv:1907.03876*, 2019.
- Mnih, V., Kavukcuoglu, K., Silver, D., Graves, A., Antonoglou, I., Wierstra, D., and Riedmiller, M. Playing atari with deep reinforcement learning. *arXiv preprint arXiv:1312.5602*, 2013.
- Nair, A., McGrew, B., Andrychowicz, M., Zaremba, W., and Abbeel, P. Overcoming exploration in reinforcement learning with demonstrations. In *2018 IEEE International Conference on Robotics and Automation (ICRA)*, pp. 6292–6299. IEEE, 2018.
- Nair, V. and Hinton, G. E. Rectified linear units improve restricted boltzmann machines. In *Proceedings of the 27th international conference on machine learning (ICML-10)*, pp. 807–814, 2010.
- Paine, T. L., Gulcehre, C., Shahriari, B., Denil, M., Hoffman, M., Soyer, H., Tanburn, R., Kapturowski, S., Rabinowitz, N., Williams, D., et al. Making efficient use of demonstrations to solve hard exploration problems. *arXiv preprint arXiv:1909.01387*, 2019.
- Paszke, A., Gross, S., Chintala, S., Chanan, G., Yang, E., DeVito, Z., Lin, Z., Desmaison, A., Antiga, L., and Lerer, A. Automatic differentiation in pytorch. 2017.
- Pfeiffer, M., Shukla, S., Turchetta, M., Cadena, C., Krause, A., Siegwart, R., and Nieto, J. Reinforced imitation: Sample efficient deep reinforcement learning for mapless navigation by leveraging prior demonstrations. *IEEE Robotics and Automation Letters*, 3(4):4423–4430, 2018.
- Pomerleau, D. A. Efficient training of artificial neural networks for autonomous navigation. *Neural computation*, 3(1):88–97, 1991.
- Rajeswaran*, A., Kumar*, V., Gupta, A., Vezzani, G., Schulman, J., Todorov, E., and Levine, S. Learning Complex Dexterous Manipulation with Deep Reinforcement Learning and Demonstrations. In *Proceedings of Robotics: Science and Systems (RSS)*, 2018.
- Reddy, S., Dragan, A. D., and Levine, S. Sqil: imitation learning via regularized behavioral cloning. *arXiv preprint arXiv:1905.11108*, 2019.
- Rhinehart, N., McAllister, R., and Levine, S. Deep imitative models for flexible inference, planning, and control. *arXiv preprint arXiv:1810.06544*, 2018.
- Silver, D., Huang, A., Maddison, C. J., Guez, A., Sifre, L., Van Den Driessche, G., Schrittwieser, J., Antonoglou, I., Panneershelvam, V., Lanctot, M., et al. Mastering the game of go with deep neural networks and tree search. *nature*, 529(7587):484–489, 2016.
- Sun, W., Bagnell, J. A., and Boots, B. Truncated horizon policy search: Combining reinforcement learning & imitation learning. In *International Conference on Learning Representations*, 2018a.
- Sun, W., Gordon, G. J., Boots, B., and Bagnell, J. Dual policy iteration. In *Advances in Neural Information Processing Systems*, pp. 7059–7069, 2018b.
- Sutton, R. S., Barto, A. G., et al. *Introduction to reinforcement learning*, volume 135. MIT press Cambridge, 1998.

Tassa, Y., Doron, Y., Muldal, A., Erez, T., Li, Y., Casas, D. d. L., Budden, D., Abdolmaleki, A., Merel, J., Lefrancq, A., et al. Deepmind control suite. *arXiv preprint arXiv:1801.00690*, 2018.

Ueltzhöffer, K. Deep active inference. *Biological cybernetics*, 112(6):547–573, 2018.

Vecerik, M., Hester, T., Scholz, J., Wang, F., Pietquin, O., Piot, B., Heess, N., Rothörl, T., Lampe, T., and Riedmiller, M. Leveraging demonstrations for deep reinforcement learning on robotics problems with sparse rewards. *arXiv preprint arXiv:1707.08817*, 2017.

Verma, A., Le, H., Yue, Y., and Chaudhuri, S. Imitation-projected programmatic reinforcement learning. In *Advances in Neural Information Processing Systems*, pp. 15726–15737, 2019.

A. Implementation

To stabilize the learning process, we adopt burn-in, a technique to recover initial states of RNN’s hidden variables h_t (Kapturowski et al., 2019). As shown in Algorithm 1, the agent calculates the Free Energy with mini batches sampled from the expert or agent dataset \mathcal{D} , which means that h_t is initialized randomly in every mini batch calculation. Since the Free Energy heavily depends on the value of h_t , it is crucial to estimate the accurate hidden states every iteration. We set a burn-in period when a portion of the mini batch data sequence is used for unrolling the networks to produce initial states of h_t . After the burn-in period, we update the networks using the remaining part of the data sequence.

We use PyTorch (Paszke et al., 2017) to write neural networks and run experiments using NVIDIA GeForce GTX 1080 Ti / RTX 2080 Ti / Tesla V100 GPU (1 GPU per experiment). The training time for our FENet implementation is about 24 hours on the DeepMind Control Suite environment. As for the hyper parameters, we use the convolutional encoder and decoder networks from (Ha & Schmidhuber, 2018) and Recurrent State Space Model from (Hafner et al., 2019b) and implement all other functions as three dense layers of size 200 with ReLU activations (Nair & Hinton, 2010). We made a design choice to make the policy prior, the policy posterior, the observation likelihood, and the reward likelihood deterministic functions while we make the state prior and the state posterior stochastic functions. We use the batch size $B = 25$ for ‘Imitation RL’ with FENet, and $B = 50$ for other types and baseline methods. We use the chunk length $L = 50$, the burn-in period 20. We use seed episodes $S = 40$, expert episodes $N = 10000$ trained with PlaNet (Hafner et al., 2019b), collect interval $C = 100$ and action exploration noise Normal(0, 0.3). We use the discount factor $\gamma = 0.99$ and the target smoothing

rate $\rho = 0.01$. We use Adam (Kingma & Ba, 2014) with learning rates $\alpha = 10^{-3}$ and scale down gradient norms that exceed 1000. We scale the reward-related loss by 100, the policy-prior-related loss by 10. We clip KL loss between the hidden states below 3 free nats and clip KL loss between the policies below 0.6.

B. Expert data collection process

We first trained PlaNet for Cheetah-run and Walker-walk. We used Soft Actor-Critic (SAC) (Haarnoja et al., 2018) for Quadruped-walk because PlaNet cannot solve Quadruped-walk very much as shown in Figure 4. Then we saved the model parameters when PlaNet or SAC achieved asymptotic performance for each task. After this, we generated 10,000 expert trajectories for each task using the saved model parameters. The suboptimal expert dataset is what we collected by using the model parameters of fewer learning iterations before reaching to asymptotic performance. For example as shown in Figure 7, the suboptimal expert in Cheetah-run is PlaNet agent that was trained halfway to reach the return of 200.